

Passive scalar transport in peripheral regions of random flows

A. Chernykh^{1,2} and V. Lebedev^{3,4}

¹ Institute of Automation and Electrometry SB RAS

² Novosibirsk State University

³ Landau Institute for Theoretical Physics RAS

⁴ Moscow Institute of Physics and Technology

We investigate statistical properties of the passive scalar mixing in random (turbulent) flows assuming weakness of its diffusion. Then at advanced stages of the passive scalar decay its unmixed residue is concentrated primarily in a narrow diffusive layer near the wall and its transport to bulk goes through the peripheral region (laminar sublayer of the flow). We conducted Lagrangian numerical simulations of the process for different space dimensions d and revealed structures responsible for the transport that are passive scalar tongues pulled from the diffusive boundary layer to bulk. We investigated statistical properties of the passive scalar and of the passive scalar integrated along the wall. Moments of both objects demonstrate scaling behavior outside the diffusive boundary layer. We propose an analytical scheme for the passive scalar statistics, explaining the features observed numerically.

PACS numbers: 05.10.-a, 05.20.-y, 05.40.-a, 47.27.-i

I. INTRODUCTION

Stochastic dynamics of such scalar fields, as temperature or concentration of pollutants, in random (turbulent) flows is of great importance in different physical contexts, from cosmology to micro-fluidics. If the back reaction of the field to the flow is negligible then the field is called passive scalar. We consider the passive scalar in random flows, where the flow velocity varies randomly in time. Theoretical examination of dynamical and statistical properties of the passive scalar in random flows goes back to classical works of Obukhov and Corrsin [1, 2], where a phenomenology for the passive scalar statistics in turbulent flows was developed in spirit of the Kolmogorov scheme [3]. Modern understanding of the passive scalar statistics in turbulent flows is reflected in Refs. [4–7], see also the books [8–10]. The mixing problem for the passive scalar is investigated for chaotic flows as well, see the book of Ottino [11]. An interesting example of a random flow is the so-called elastic turbulence, discovered by Groisman and Steinberg [12] in polymer solutions. Observations of the passive scalar statistics in the elastic turbulence were reported in Ref. [13].

In 90th, a series of theoretical works devoted to the passive scalar statistics was done in the framework of the so-called Kraichnan model where the turbulent flow is assumed to be short correlated in time and possessing a definite scaling. The works enabled one to reveal general features of the passive scalar statistics in turbulent flows including the so-called anomalous scaling and intermittency [14–16], see also the surveys [17, 18]. However, the approach implies spacial homogeneity of the flow statistics and is not, consequently, directly applicable to regions near walls.

In this paper we investigate the passive scalar statistics in peripheral regions of a vessel where the developed (high-Reynolds) turbulence is excited. Speaking about

the peripheral regions of the turbulent flows, we imply a laminar (viscous) sublayer formed near walls where the velocity field can be regarded as smooth, it varies on distances of the order of the thickness of the sublayer. However, the velocity remains a random function of time there. Some laminar boundary layer is characteristic also of the elastic turbulence [19]. The passive scalar statistics in the peripheral region is determined by a complicated interplay of its diffusion and random advection in highly anisotropic situation caused by presence of the walls.

We are interested in advanced stages of the passive scalar decay assuming that the Peclet or the Schmidt number is large. In the case the unmixed fraction of the passive scalar is located mainly in a narrow diffusive layer near the wall, thinner than the thickness of the peripheral region [20]. Then the passive scalar transport to bulk goes through the peripheral region outside the diffusive layer. Just this peripheral region plays a crucial role in formation of statistical characteristics of the passive scalar transport. The same reasoning can be applied to a stationary case related, say, to a permanent heat flow going from the walls through the periphery region to bulk. Moreover, fast chemical reactions can be analyzed inside the same scheme, see Ref. [21]. A theoretical approach to the problem was developed in Ref. [22], principal predictions of the theory were confirmed by experiment, see Ref. [23].

To check the theoretical predictions in detail, we conducted extensive numerical simulations of the problem based on Lagrangian dynamics of particles representing the passive scalar. Aiming to establish main qualitative properties of the passive scalar transport in the peripheral regions, we focused on the $2d$ (two-dimensional) case. However, a big advantage of the Lagrangian scheme is an ability to extend the approach without essential troubles to higher dimensions. We performed simulations for the space dimensionalities $d = 3 \div 5$ to establish universal-

ity of the passive scalar statistical behavior in $2d$ and to reveal features characteristic of higher dimensions. We used a scheme with permanent injection of particles near the wall that produces statistically homogeneous in time statistics of the passive scalar. However, our conclusions are correct for the decaying case as well because of adiabaticity: events responsible for the passive scalar transport to bulk are much faster than the average passive scalar decay.

The obtained numerical data can be used to compute averages characterizing the passive scalar statistics. First of all, we found moments of the passive scalar at different separations from the wall. The data show an existence of a well pronounced diffusive layer where the passive scalar is mainly concentrated, in accordance with the theoretical expectations formulated in Ref. [22]. Outside the diffusive layer the passive scalar moments demonstrate scaling behavior with exponents deviating from ones proposed in Ref. [22] where diffusion was assumed to be negligible outside the diffusive layer. We checked that the deviations are related to diffusion, indeed. The situation resembles the passive scalar statistics in the Batchelor velocity field on scales larger than the pumping length where diffusion appears to be relevant [24], that corrects the diffusionless behavior examined in Ref. [25]. Next, we introduced the passive scalar integrated along a surface parallel to the wall. The diffusion along the wall drops from the equation for the object. We demonstrated numerically that outside the diffusive layer moments of the integral passive scalar have well pronounced scaling behavior, as a function of separation from the wall. We found the corresponding scaling exponents for moments with degrees $n = 1 \div 6$ in space dimensionalities $d = 2 \div 5$. The moments exhibit an anomalous scaling signalling about strong intermittency of the passive scalar statistics.

The simulations enabled us to reveal objects lying behind the intermittency. The objects are tongues of the passive scalar pulled from the diffusive layer towards bulk. The tongue cross section diminishes as the separation from the wall increases (due to increasing the velocity component perpendicular to the wall). That explains why diffusion can play an essential role even in the region outside the diffusive layer. The subsequent tongue evolution including tongue folds produces long-living structures possessing complex shape. Sometimes the tongues are pulled so strongly that push irreversibly a passive scalar portion away from the wall. Just this mechanism is responsible for the passive scalar transport to bulk, that naturally explains its strong intermittency.

We suggest a theoretical scheme for explanation of the passive scalar statistics, based on smallness of the passive scalar correlation length along the wall outside the diffusive layer. The scheme enables one to find explicit expressions for scaling exponents characterizing different objects. A comparison of the theoretical predictions with numerics shows that they agree satisfactory. Some preliminary results of our work were published in Ref. [26].

The structure of the paper is as follows. In the second section we present our theoretical approach concerning the passive scalar dynamics and statistics in the peripheral region and propose a scheme giving the scaling exponents. In the third section we explain our computational scheme, present computed moments of the passive scalar and integral passive scalar, give a description of the passive scalar tongues, and compare our numerical results with theory. In Conclusion we give an outline of our results, their possible applications and directions of future investigations.

II. THEORETICAL DESCRIPTION

We consider the passive scalar statistics in peripheral regions of a random flow, that are regions near boundaries (walls). Our principal example is the viscous (laminar) boundary layer of the developed high-Reynolds hydrodynamic turbulence (see, e.g., the book [8]). However, our approach can be applied to other situations. For example, one can think about the peripheral region of the elastic turbulence [12]. The only feature relevant for us is smoothness of the flow in the boundary layer, whereas the velocity varies randomly in time there.

We designate the passive scalar field as θ . It can represent both, temperature variations or concentration of pollutants. The passive scalar evolution (decay) in an external flow is described by the advection-diffusion equation

$$\partial_t \theta + \mathbf{v} \nabla \theta = \kappa \nabla^2 \theta, \quad (1)$$

where \mathbf{v} is the flow velocity and κ is the diffusion (thermodiffusion) coefficient. Below, the fluid is assumed to be incompressible (that is the flow is divergentless, $\nabla \mathbf{v} = 0$). The equation (1) implies that there are no sources of the passive scalar in the volume. However, we do not exclude a passive scalar flux from the vessel walls.

The equation (1) has to be supplemented by boundary conditions at the wall. If θ is the density of pollutants and the wall is impenetrable for the pollutants then the gradient of θ in the direction perpendicular to the wall is zero near the wall, that corresponds to zero pollutant flux to the boundary. In the case we deal with the passive scalar decay, leading ultimately to its homogeneous distribution in space. If θ is temperature then its gradient in the direction perpendicular to the wall can be non-zero, that corresponds to finite heat flux through the boundary (from the wall). If walls are made of a well heat conducting material then a value of θ (temperature) has to be regarded as fixed at the boundary.

We assume that the Peclet or the Schmidt number is large (that is the diffusion coefficient κ is small in comparison with the fluid kinematic viscosity ν). Then, as it was demonstrated in the work [22], the passive scalar dynamics in the peripheral region is slow in comparison with the velocity dynamics. Therefore the passive scalar

is rapidly mixed in bulk (for a time that can be estimated as an inverse Lyapunov exponent of the flow) that leads to a homogeneous spacial distribution of the passive scalar, $\theta = \text{const}$. The subsequent passive scalar evolution is related mainly to the peripheral regions that supply bulk by passive scalar fluctuations. We assume that bulk can be treated as a big reservoir, then the bulk homogeneous value of θ , θ_b , can be regarded as independent of time. Below, we imply that the passive scalar field is shifted by θ_b , that leads to the condition $\theta \rightarrow 0$ as we pass from the periphery to bulk.

A. Correlation Functions

Statistical properties of the passive scalar can be described in terms of its correlation functions

$$F_n(t, \mathbf{r}_1, \dots, \mathbf{r}_n) = \langle \theta(t, \mathbf{r}_1) \dots \theta(t, \mathbf{r}_n) \rangle, \quad (2)$$

where angular brackets mean averaging over large times (larger than the velocity correlation time). Since the velocity tends to zero at approaching the wall and the molecular diffusion is assumed to be weak, the passive scalar dynamics, determined by an interplay of the advection and diffusion, is slower than the velocity dynamics in the peripheral region. Therefore at investigating the passive scalar dynamics the velocity can be regarded as short correlated in time and closed equations can be derived for the passive scalar correlation functions (see, e.g., [18, 22])

$$\begin{aligned} \partial_t F_n &= \kappa \sum_{m=1}^n \nabla_m^2 F_n \\ &+ \sum_{m,k=1}^n \sum_{\alpha\beta} \partial_{m\alpha} [D_{\alpha\beta}(\mathbf{r}_m, \mathbf{r}_k) \partial_{k\beta} F_n], \end{aligned} \quad (3)$$

where the object $D_{\alpha\beta}$ is expressed via the pair velocity correlation function as

$$D_{\alpha\beta}(\mathbf{r}_1, \mathbf{r}_2) = \int_0^\infty dt' \langle v_\alpha(t+t', \mathbf{r}_1) v_\beta(0, \mathbf{r}_2) \rangle. \quad (4)$$

Here, again, angular brackets mean averaging over times larger than the velocity correlation time.

The structure of the equation (3) is quite transparent: the evolution of the passive scalar correlation functions is determined by the molecular diffusion (the first term in the right-hand side) and by the eddy diffusion (the second term in the right-hand side). Therefore the quantity $D_{\alpha\beta}$ can be called the eddy diffusion tensor, since it describes diffusion of the passive scalar related to the random flow. This effect can be compared with the turbulent diffusion of the passive scalar in turbulent flows in bulk on scales larger than the viscous length. However, in our case the eddy diffusion tensor $D_{\alpha\beta}$ is associated with a smooth flow, and can be used for description of the passive scalar dynamics on scales smaller than the turbulent viscous length.

We assume that the walls of the vessel are smooth and that the boundary layer width is much less than the curvature radii of the wall. Then it can be treated as flat in the main approximation. Let us introduce a reference system with the Z -axis perpendicular to the wall and assume that the fluid occupies the region $z > 0$. Smoothness of the velocity leads to the proportionality laws $v_x, v_y \propto z$ and $v_z \propto z^2$ for the velocity components along and perpendicular to the wall, respectively. The laws are consequences of the velocity smoothness, of the non-slipping boundary condition $\mathbf{v} = 0$ at the wall, and of the incompressibility condition $\nabla \mathbf{v} = 0$.

Below we assume that the velocity statistics is homogeneous in time, and also assume its homogeneity along the wall. Due to the assumed homogeneity, velocity correlation functions are dependent on time differences and on differences of the coordinates x and y . Say, the eddy diffusion tensor (4) is independent of time and does depend on differences $x_1 - x_2$ and $y_1 - y_2$. However, it depends on both z_1 and z_2 due to the strong inhomogeneity of the system in the direction perpendicular to the wall. A z -dependence of the eddy diffusion tensor components can be found directly from the proportionality laws $v_x, v_y \propto z$ and $v_z \propto z^2$. Say,

$$D_{zz}(x, y, z_1; x, y, z_2) = \mu z_1^2 z_2^2, \quad (5)$$

where μ is a constant characterizing strength of the velocity fluctuations in the peripheral region.

The equation for the first moment of θ (average value of the passive scalar field), $\langle \theta \rangle$, is

$$\partial_t \langle \theta \rangle = \partial_z [\mu z^4 \partial_z \langle \theta \rangle] + \kappa \partial_z^2 \langle \theta \rangle, \quad (6)$$

as it follows from Eqs. (3,5). Comparing the advection and the diffusion terms in the equation (6) one finds a characteristic diffusion length r_{bl} defined as

$$r_{bl} = (\kappa/\mu)^{1/4}. \quad (7)$$

The quantity determines the thickness of the diffusion boundary layer formed near the wall. Due to smallness of κ (remind that the Peclet or the Schmidt number is assumed to be large) the diffusion length is much less than the thickness of the peripheral region, where the law $v_z \propto z^2$ is satisfied.

We consider an advanced stage of the passive scalar decay or a statistically stationary situation caused by the permanent passive scalar flux through the wall. Then the passive scalar θ is non-zero primarily in the diffusive boundary layer, at $z \lesssim r_{bl}$ (remind that after subtraction of its bulk value the field θ should tends to zero in bulk that is at $z \rightarrow \infty$). However, we are interested mainly in the passive scalar transport through the region $z \gg r_{bl}$, where the passive scalar is carrying from the diffusive boundary layer to bulk. There it is possible to neglect the molecular diffusion term in Eq. (6) and we arrive at the proportionality law

$$\langle \theta \rangle \propto z^{-3}, \quad (8)$$

that gives the decaying rate of the average θ as z grows. Note that the law (8) corresponds to a constant average passive scalar flow through the planes $z = \text{const}$, that is the flux is independent of z .

One anticipates that at $z \gg r_{bl}$ high passive scalar moments possess some scaling behavior as well as $\langle \theta \rangle$. We introduce the corresponding scaling exponents

$$\langle \theta^n \rangle \propto z^{-\eta_n}, \quad (9)$$

If the molecular diffusion is irrelevant outside the diffusion boundary layer then $\eta_n = 3$ [22]. However, our numerical data imply that the molecular diffusion is relevant even at $z \gg r_{bl}$ (below we give an explanation of the phenomenon). Therefore the exponents η_n are not equal to 3 and their values are subject of a special investigation.

Let us turn to the passive scalar correlation functions (2). At $z \gg r_{bl}$ their dependence on the coordinates along the wall are characterized by a correlation length l , that can be found by balance of the molecular and the eddy diffusion along the wall. The eddy diffusivity term in Eq. (3) can be estimated as μz^2 , see Eq. (5), the law $\propto z^2$ follows from the z -dependence of the velocity components. Comparing the molecular diffusion term $\sim \kappa/l^2$ and the eddy diffusion term in Eq. (3), one finds

$$l \sim \sqrt{\kappa/\mu} z^{-1}. \quad (10)$$

The quantity is of the order of r_{bl} at $z \sim r_{bl}$ and diminishes $\propto z^{-1}$ as z grows.

B. Integral Passive Scalar

To exclude effects of the molecular diffusion, we introduce an integral of the passive scalar field along a surface parallel to the wall

$$\Theta(t, z) = A^{-1} \int dx dy \theta(t, x, y, z), \quad (11)$$

where A is the area of the surface and z is its separation from the wall. We designate correlation functions of the object as

$$\Phi_n(t, z_1, \dots, z_n) = \langle \Theta(t, z_1) \dots \Theta(t, z_n) \rangle. \quad (12)$$

Integrating Eq. (3) over x_k and y_k , one obtains

$$\partial_t \Phi_n = \kappa \sum_{m=1}^n \partial_{mz}^2 \Phi_n + \int dx_1 \dots dx_n dy_1 \dots dy_n \left\{ \sum_{m,k=1}^n \partial_{mz} [D_{zz} \partial_{kz} F_n] + \sum_{m \neq k} \partial_{mz} [(\partial_{kz} D_{zz}) F_n] \right\}, \quad (13)$$

where $D_{zz} = D_{zz}(\mathbf{r}_m, \mathbf{r}_k)$. At deriving Eq. (13) we have taken some integrals in part and used the constraint

$$\frac{\partial}{\partial x_k} D_{zx}(\mathbf{r}_m, \mathbf{r}_k) + \frac{\partial}{\partial y_k} D_{zy}(\mathbf{r}_m, \mathbf{r}_k) + \frac{\partial}{\partial z_k} D_{zz}(\mathbf{r}_m, \mathbf{r}_k) = 0,$$

which is a consequence of the incompressibility condition $\nabla \mathbf{v} = 0$.

One expects a scaling behavior of the correlation functions (12) at $z \gg r_{bl}$. Then the last term in Eq. (13) can be estimated as $\mu z^4 \partial_z^2 \Phi$. Consequently, the term with the molecular diffusion κ in Eq. (13) can be neglected in the region. The argumentation is the same as was used for the moment $\langle \theta \rangle$, where the law (8) was derived from Eq. (6). Note also, that in the decaying case the time derivative in Eq. (13) can be estimated as $\kappa/r_{bl}^2 = \sqrt{\kappa\mu}$, the term is much less than $\mu z^4 \partial_z^2 \sim \mu z^2$ at $z \gg r_{bl}$. Therefore the term with the time derivative can be neglected in the region as well, and we obtain quasi-stationary equations for Φ_n . That reflects adiabaticity of the passive scalar statistics.

It is reasonable to assume that the correlation function $F_n(t, \mathbf{r}_1, \dots, \mathbf{r}_n)$ is correlated along the $X - Y$ plane on distances of the order of the correlation length l (10) that is much smaller than the characteristic velocity length (width of the peripheral region), then D_{zz} in Eq. (13) can be substituted by $\mu z_m^2 z_k^2$. Then we obtain closed equations for the correlation functions

$$\begin{aligned} \partial_t \Phi_n(t, z_1, \dots, z_n) = & \mu \sum_{m,k=1}^n \frac{\partial}{\partial z_m} \left(z_m^2 z_k^2 \frac{\partial}{\partial z_k} \Phi_n \right) \\ & + 2\mu \sum_{m \neq k} \frac{\partial}{\partial z_m} (z_m^2 z_k \Phi_n), \end{aligned} \quad (14)$$

where we omitted the molecular diffusion term (see the above argumentation).

The equations (14) lead to the following closed equations for the moments of the integral passive scalar

$$\partial_t \langle \Theta^n \rangle = \mu [z^4 \partial_z^2 + 4nz^3 \partial_z + 4n(n-1)z^2] \langle \Theta^n \rangle. \quad (15)$$

In the stationary (or quasi-stationary) case (where $\partial_t \langle \Theta^n \rangle$ is negligible) we obtain a homogeneous differential equation for the n -th moment that admits a power solution

$$\langle \Theta^n \rangle \propto z^{-\zeta_n}. \quad (16)$$

The exponents ζ_n can be easily found from Eq. (15), they are

$$\zeta_n = 2n - 1/2 + \sqrt{2n + 1/4}. \quad (17)$$

We have chosen the positive sign of the square root leading to the reference value $\zeta_1 = 3$, as it should be in accordance with Eq. (8). We observe anomalous scaling, that is a non-linear dependence of ζ_n on n , that can be compared with the anomalous scaling of the passive scalar in the Kraichnan model [14–16].

A natural conjecture that enables one to relate the moments of the passive scalar θ and those of the integral passive scalar Θ is in using the passive scalar correlation length l as a recalculation factor. Then we come to an estimation

$$\langle \Theta^n \rangle \sim \frac{l^{(d-1)(n-1)}}{A^{n-1}} \langle \theta^n \rangle. \quad (18)$$

Here d is dimensionality of space, that is equal to 3 in real flows but can be arbitrary in numerical simulations. The estimation (18) together with Eq. (10) lead to the relation

$$\eta_n = \zeta_n - (n-1)(d-1), \quad (19)$$

between the exponents introduced by Eqs. (9,16).

III. SIMULATIONS

We conducted Lagrangian simulations where dynamics of a large number of particles subjected to flow advection and Langevin forces (producing diffusion) is examined. The set of the particles is used instead of the passive scalar field θ , that can be interpreted as density of the particles. A big advantage of the approach is its applicability to different space dimensions d . Indeed, in the scheme the number of variables (coordinates of the particles) grows as a power of d (at a given number of the particles), but not exponentially.

To establish principal qualitative features of the passive scalar transport, we perform mainly $2d$ simulations. The setup is periodic in x (coordinate along the wall) with a period L . In majority of simulations the velocity field is chosen to be

$$v_x = z \left(\xi_1 \cos \frac{2\pi x}{L} + \xi_2 \sin \frac{2\pi x}{L} \right) \frac{L}{\pi}, \quad (20)$$

$$v_z = z^2 \left(\xi_1 \sin \frac{2\pi x}{L} - \xi_2 \cos \frac{2\pi x}{L} \right), \quad (21)$$

where ξ_1 and ξ_2 are independent random functions of time. Let us stress, that the velocity field (20,21) satisfies the incompressibility condition $\partial_x v_x + \partial_z v_z = 0$ for any functions $\xi_1(t)$ and $\xi_2(t)$. They are chosen to possess identical Gaussian probability distributions, then the velocity field (20,21) has statistics homogeneous in x (along the wall). In our numerics, we have chosen $L = 10$.

Though in reality the proportionality laws $v_x \propto z$ and $v_z \propto z^2$ are satisfied inside the laminar boundary layer, in our setup the expressions for the velocity components like (20,21) are formally used at all z , that is bulk corresponds to $z = \infty$. However, the law $v_z \propto z^2$ implies that the particles may reach the z -infinity for a finite time. That ensures a finite particle flux to bulk since sometimes a finite number of particles passages there. Therefore the passive scalar transport to bulk is well defined in our setup.

Since the velocity correlation time in the peripheral region is much less than the passive scalar mixing time, one should consider $\xi_1(t)$ and $\xi_2(t)$ as white noises. However, in computer simulations one cannot realize zero correlation time. We model the functions by telegraph processes, where both functions, ξ_1 and ξ_2 , remain constants inside time slots of a small duration τ , and the values of ξ_1 and ξ_2 inside the slots are chosen to be random variables with identical normal distributions. An example of

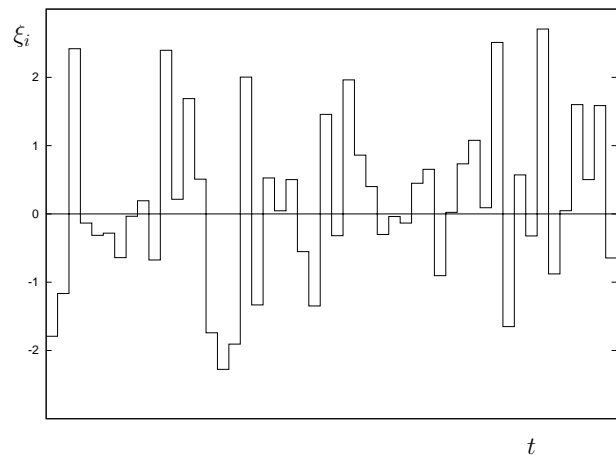


FIG. 1: An example of the telegraph process.

such telegraph process is plotted in Fig. 1. In our simulations the averages were $\langle \xi_1^2 \rangle = \langle \xi_2^2 \rangle = 1$ and different slot sizes were used, $\tau = 0.001; 0.002; 0.004$. Then, in accordance with the definition (5), $\mu = \tau/2$.

In our scheme a particle trajectory $\mathbf{q}(t)$ obeys the equation

$$\partial_t \mathbf{q} = \mathbf{v}(t, \mathbf{q}) + \boldsymbol{\zeta}(t), \quad (22)$$

where the first term represents the particle advection and the second term represents the Langevin force. Let us stress that the variables $\boldsymbol{\zeta}$ are independent for different particles whereas the variables ξ_1 and ξ_2 are identical for all particles, according to physical meaning of the variables. The Langevin force $\boldsymbol{\zeta}$ is also modeled by a telegraph process with the same time slot duration τ and with normal distributions of the values in the slots. To ensure a given value of the diffusion coefficient κ , one should choose

$$\langle \zeta_x^2 \rangle = \langle \zeta_z^2 \rangle = 2\kappa/\tau. \quad (23)$$

In majority of simulations we have chosen $\kappa = \tau/2$, and therefore the diffusive length was $r_{bl} = 1$, in accordance with the definition (7).

Inside a time slot all the variables, ξ_1 , ξ_2 and $\boldsymbol{\zeta}$, are time-independent constants and the equation (22) becomes an autonomous ordinary differential equation. It was solved as follows. A time slot was divided into a number of time intervals and the equation was solved (without the Langevin force) using the second order Runge-Kutta method. The number of intervals is z -dependent, it is proportional to z at $z > 2.5$. For $z > 12$ we solved equations for $1/\varrho_z$ instead of ϱ_z . Both features are motivated by the strong dependence of the velocity on z , $v_z \propto z^2$. After solving the equation inside a slot a term produced by the Langevin force was added. To examine role of diffusion outside the diffusive boundary layer, in some simulations we switched off the diffusion (the Langevin forces) at distances $z > z_d$ (where a choice of z_d is different for different cases).

The particles are permanently injected near the wall in random positions at the beginning of each time slot. The simulations were performed in the stripe $0 < z < 100$, the particles crossing the lines $z = 0$ and $z = 100$ were excluded from the set. The number of particles leaving the region $0 < z < 100$ through the wall is much larger than the number of particles escaping through the line $z = 100$. The last ones correspond to the passive scalar transport to bulk. A balance between the particle injection and losses leads to a statistical equilibrium achieved gradually in the numerics. Thus, our simulations cover the statistically stationary passive scalar transport. It corresponds both to the steady temperature distribution supported by a constant heat flux from the wall and to the decay of the concentration of pollutants that can be treated adiabatically.

An extension of our scheme to higher dimensions, $d > 2$, is straightforward. We utilize the same equation (22) where all quantities have d components. The Langevin forces ζ are determined by the same relations (23) and a generalization of the expressions (20,21) is as follows. The velocity \mathbf{v} is determined by a set of $2(d-1)^2$ random variables ξ_{1ij} and ξ_{2ij} :

$$v_i = z \sum_{j=1}^{n-1} \left(\xi_{1ij} \cos \frac{2\pi x_j}{L} + \xi_{2ij} \sin \frac{2\pi x_j}{L} \right) \frac{L}{\pi}, \quad (24)$$

$$v_z = z^2 \sum_{j=1}^{n-1} \left(\xi_{1jj} \sin \frac{2\pi x_j}{L} - \xi_{2jj} \cos \frac{2\pi x_j}{L} \right), \quad (25)$$

where the subscripts i, j numerate first $d-1$ space coordinates and the last d -th coordinate is z . Here, all ζ , ξ_{1ij} and ξ_{2ij} are, again, telegraph processes with the same statistical properties as above, and we use the second-order Runge-Kutta scheme inside a time slot.

In terms of the particles, the passive scalar field θ is defined as a number of particles per unit volume, that is as a number of particles inside a box divided by the box volume. Of course, the definition works well provided the box is small (in comparison with all characteristic scales of the problem) and the number of particles inside the box is large. To satisfy these contradictory conditions one should deal with a large enough total number of particles. That is why the injection rate in our numerics is chosen to produce a large number of particles, $10^5 \div 10^6$, in the statistical equilibrium.

A. Tongues

Our simulations shown that the passive scalar transport to bulk is related to specific structures of the passive scalar. The passive scalar is concentrated mainly in the narrow diffusive layer near the wall. However, sometimes a fluid jet is generated carrying the passive scalar from the wall towards bulk, that produces a passive scalar tongue with width (cross-section) diminishing as z grows. The property is a consequence of the law $v_z \propto z^2$ reading

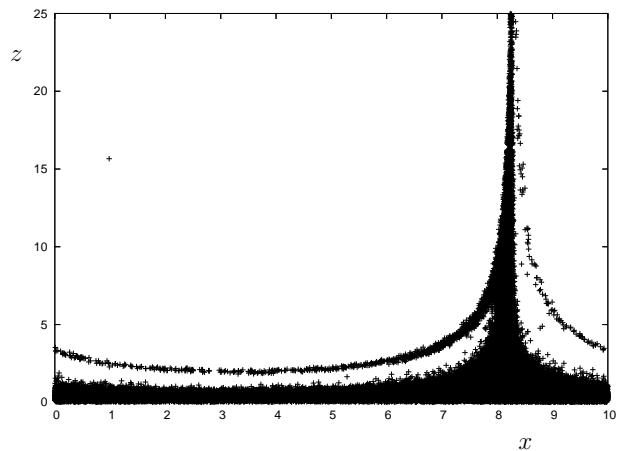


FIG. 2: An example of a passive scalar structure formed near the wall in the $2d$ random flow. Different particles are designated by small crosses.

that the z -component of the tongue velocity increases as z grows. Thus we come to a geometrical interpretation of the passive scalar correlation length l : it is the characteristic size of the tongue cross-section (taken along the wall). The cross-section behavior corresponds to an expected decrease of the correlation length as z grows. Let us stress that in accordance with Eq. (10) the characteristic tongue cross section is dependent on the diffusion coefficient κ .

A tongue is typically pulled from a “bump” of the passive scalar distribution. After some time the tongue is tilted and then pressed back to the diffusive layer. Then next tongue is pulled, usually from the bump remaining at bottom of the previous tongue, and is, in turn, pressed back to the diffusive layer. As a result, a complicated multi-fold structure is formed, an example of such structure is drawn in Fig. 2, that represents a snapshot generated in our simulations.

Sometimes the tongue is pulled upto z -infinity, and then a portion of the passive scalar (a number of particles) is pushed to bulk. After that the tongue is tilted and the passive scalar current to bulk stops. That implies that the passive scalar flux, $\int dx \theta v_z$ in $2d$, is highly intermittent quantity at $z > r_{bl}$. The conclusion is confirmed by the flux histograms drawn in Fig. 3 for different z . In simulations, the passive scalar flux was measured as a number of particles crossing the plain $z = \text{const}$ during a time τ . At $z = 0$ the flux probability distribution is practically Gaussian, being formed by a balance between the random injection of the particles and their leaving the wall. However, the distribution becomes less and less Gaussian as z grows. The histograms in Fig. (3) are practically symmetric. The property is related to the fact that only a small amount of particles in the tongue are pulled to bulk, the majority of particles returns back, that produces practically equal fluxes to bulk and toward the wall. That explains why at $z \gg r_{bl}$ the root mean-square fluctuation of the flux is much larger than

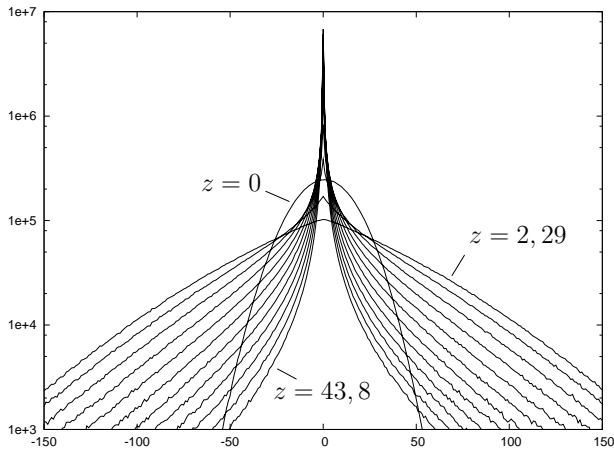


FIG. 3: Histograms of the passive scalar flux at different separations from the wall. The root mean square fluctuations are much larger than the average value and the histograms are practically symmetric. At $z = 0$ the probability distribution is Gaussian whereas at $z > r_{bl}$ it has exponential tails.

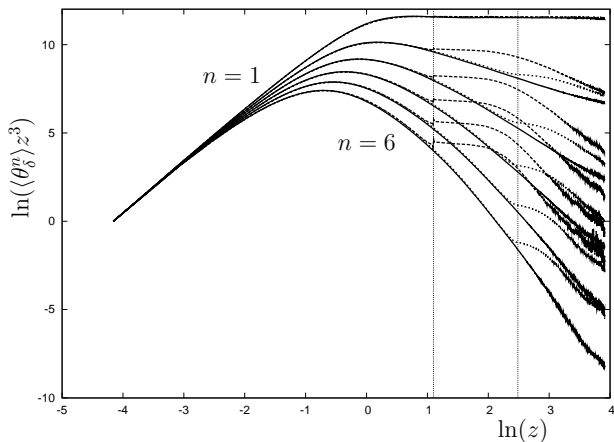


FIG. 4: Log-log plot of the moments of θ_δ , $\langle \theta_\delta^n \rangle$, multiplied by z^3 , for $\delta = 0.03125$ and $n = 1 \div 6$. The graph reflects simulations where diffusion occurs everywhere, and is switched off at $z = 3$ or $z = 12$.

its average value.

B. Moments

Based on numerical data one can compute moments and correlation functions of different quantities characterizing the passive scalar statistics. One can consider both local functions or integral objects. All the quantities are computed as time averages.

We introduce an object θ_δ that is a number of particles inside a square box of size δ divided by its area δ^2 (in $2d$). The quantity θ_δ is close to θ provided the number of particles is large and the size of the box is small enough. Moments M_n of the quantity θ_δ , $M_n = \langle \theta_\delta^n \rangle$, for $n = 1 \div 6$ are computed as averages over time intervals $10^6 \div$

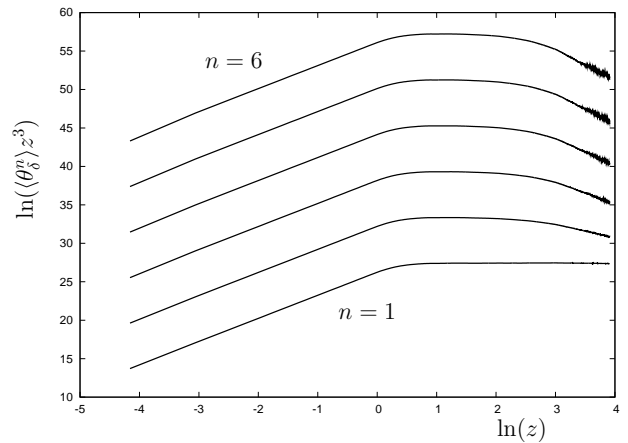


FIG. 5: Log-log plot of the moments of θ_δ , $\langle \theta_\delta^n \rangle$, multiplied by z^3 , for $\delta = 0.03125$ and $n = 1 \div 6$ in the case where diffusion is substituted by a constant velocity carrying the particles from the wall.

$10^7 \tau$ as $\delta = 0.03125$. The results are presented in Fig. 4 where the moments multiplied by z^3 are plotted in log-log coordinates (solid curves). We see that the prediction (8) for the first moment is perfectly satisfied whereas higher moments deviate strongly from the diffusionless law $\propto z^{-3}$. We conclude that the diffusion is relevant at $z > r_{bl}$, indeed.

To verify the conclusion we repeated the simulations switching off diffusion at $z > 3$ and at $z > 12$. Results are presented in Fig. 4 by dashed curves. We see an appearance of plateaus, starting just from $z = 3$ or $z = 12$ and corresponding to the law $\propto z^{-3}$, in accordance with Ref. [22]. The plateaus are observed in restricted regions of separations from the wall z slightly diminishing as n grows. An explanation of the fact is that cutoffs of the plateaus are observed where δ becomes of the order of the passive scalar correlation length (along the wall). To check this conjecture we repeated the simulations for larger values of δ and observed that the plateaus shrink as δ grows. That confirms our explanation. To be absolutely sure that the diffusion is relevant we performed simulations without diffusion but with adding a constant velocity V carrying the particles away the wall. Results of the simulations are presented in Fig. 5 where the moments $\langle \theta_\delta^n \rangle$, multiplied by z^3 , are plotted. We see plateaus signalling that outside the boundary layer the passive scalar moments behave in accordance with the diffusionless prediction.

The next object of our investigation is the integral quantity Θ that is the passive scalar integrated along the wall, see the definition (11). In numerics it is determined by a number of particles in a slice of thickness δ , parallel to the wall, divided by its volume (area), we designate the ratio as Θ_δ . In our $2d$ setup the area is equal to $L\delta$, where δ is chosen to be much less than z . The moments of Θ_δ , $\langle \Theta_\delta^n \rangle$, are computed by time averaging over a long time $\sim 10^7 \tau$. To check robustness of

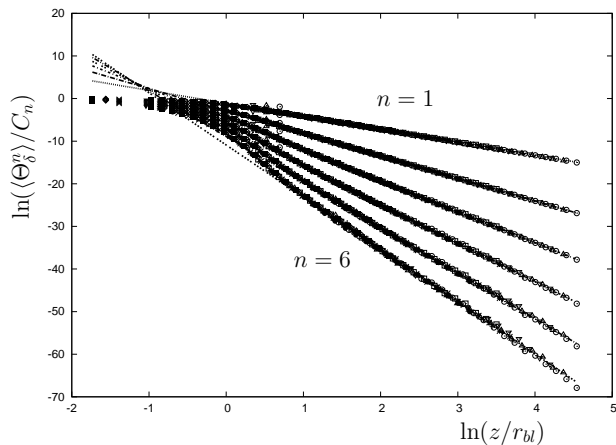


FIG. 6: Moments of Θ_δ in log-log coordinates, $n = 1 \div 6$. In the region $z > r_{bl}$ the results collapse onto single curves for three times $\tau = 0.001, 0.002, 0.004$ and four different values of the diffusion coefficient.

the results we performed computations for different time slots, $\tau = 0.001, 0.002, 0.004$, and for four different values of the diffusion coefficient κ . The figure 6 demonstrates that the values of each moment collapse to a single curve in the logarithmic coordinates $\ln(z/r_{bl})$ and $\ln(\langle \Theta_\delta^n \rangle / C_n)$ where the factors C_n are the corresponding moments near the wall.

One can check that, in accordance with our theoretical expectations, the moments of Θ_δ are insensitive to diffusion. To illustrate the assertion we present in Fig. 7 the moments of Θ_δ computed at $\tau = 0.002$ for two cases: in the first case the diffusion occurs everywhere and in the second case it is switched off at $z > 3$. One can observe no difference between the data. One can also try to use an alternative to the expression (20,21) velocity field. There are two series of data plotted in Fig. 7 and corresponding to the velocity (20,21) and to the velocity with four random factors

$$\frac{\pi v_x}{Lz} = \xi_1 \cos \frac{2\pi x}{L} + \xi_2 \sin \frac{2\pi x}{L} + \xi_3 \cos \frac{4\pi x}{L} + \xi_4 \sin \frac{4\pi x}{L}, \quad (26)$$

$$\frac{v_z}{z^2} = \xi_1 \sin \frac{2\pi x}{L} - \xi_2 \cos \frac{2\pi x}{L} + 2\xi_3 \sin \frac{4\pi x}{L} - 2\xi_4 \cos \frac{4\pi x}{L}. \quad (27)$$

Again, there is no visible difference between the series.

We observe that the moments of Θ are decreasing functions of z that are power-like in the region $z > r_{bl}$. Extracting the scaling exponents ζ_n , see the definition (17), for $n = 1 \div 6$ in $2d$ we obtain values that are presented in Fig. 8 as the lower set of points (some smooth curve is drawn through the points for better visualization). We conducted analogous simulations for higher dimensions, upto $d = 5$. The results are depicted in the same figure 8. We see that the exponents ζ_n depend on d , however,

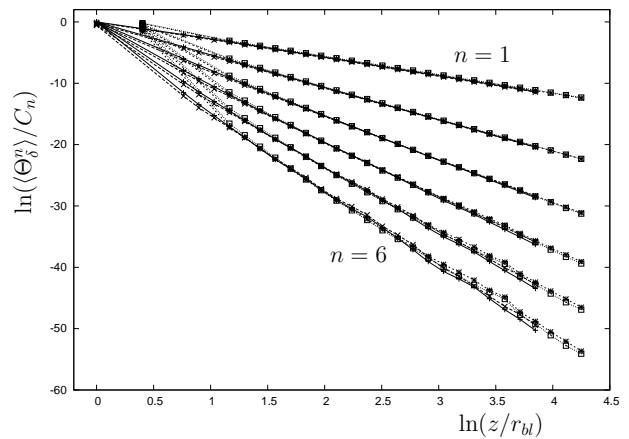


FIG. 7: Moments of Θ_δ in log-log coordinates, $n = 1 \div 6$. The results are obtained for two cases where the diffusion occurs everywhere and where it is switched off at $z > 3$, and also for two different velocity fields: with two and four harmonics.

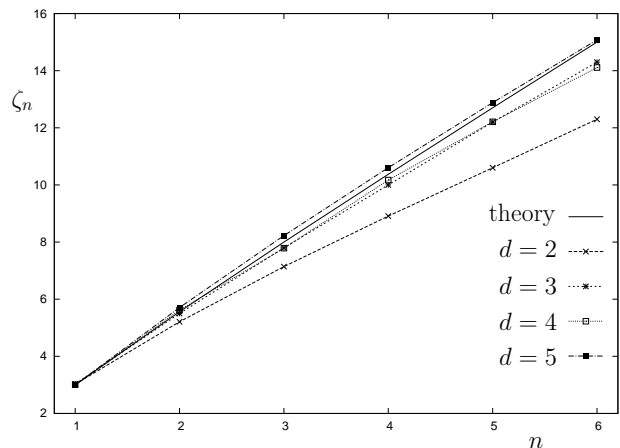


FIG. 8: Exponents of the moments $\langle \Theta_\delta^n \rangle$, for $n = 1 \div 6$ and space dimensions $d = 2 \div 5$. For comparison the theoretical curve $\zeta_n = 2n - 1/2 + \sqrt{2n + 1/4}$ is plotted (solid line).

for $d \geq 3$ they are close to the theoretical values (17) represented by a solid line.

One can think that the deviations from the theoretical values (17) are related to an existence of additional passive scalar (relatively long) correlations along the wall that can be produced by the multi-fold structures of the type drawn in Fig. 2. The long correlations should lead to increasing moments of the passive scalar in comparison with the short correlated case. It is naturally to expect that the fold effect becomes less pronounced in higher dimensions. Indeed, Fig. 8 shows that the deviations from the values (17) diminish as the space dimensionality d grows. That confirms our explanation.

To check our conjecture, we conduct simulations for the velocity field containing, like the expressions (26,27), a set of harmonics in terms of the period L : the ninth, tenth and eleventh ones. In such velocity field correlations related to the multi-fold tongue structures have

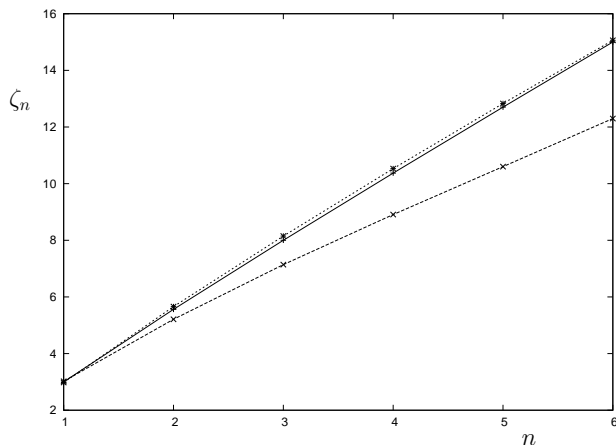


FIG. 9: Exponents of the moments $\langle \Theta_\delta^n \rangle$, for $n = 1 \div 6$ and space dimensions $d = 2$ for two different velocity fields: containing only first harmonic and three (ninth, tenth and eleventh) harmonics. For comparison the theoretical curve $\zeta_n = 2n - 1/2 + \sqrt{2n + 1/4}$ is plotted (solid line).

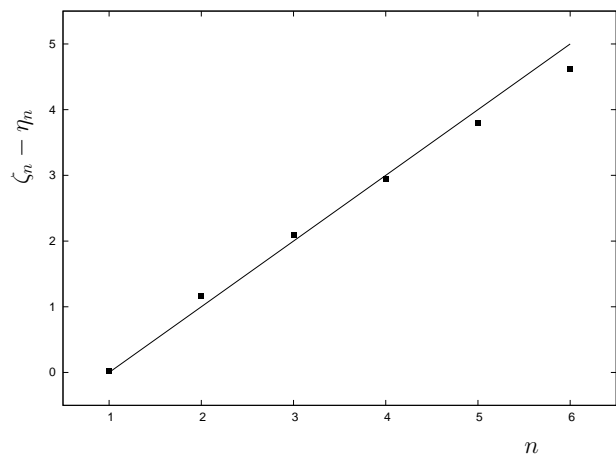


FIG. 10: The difference of the scaling exponents of moments for the integral passive scalar and for the passive scalar, $\zeta_n - \eta_n$, computed at $\delta = 0.03125$ in $2d$. For comparison, the theoretical prediction $n - 1$ is drawn.

to be suppressed, and, consequently, the exponents ζ_n should be close to the theoretical values (17). This expectation is confirmed by our simulations, the results are presented in Fig. 9, where measured exponents are plotted. We see a good agreement of the measured and theoretical exponents.

One can extract from our numerical data the exponents η_n of the moments of θ_δ , see the definition (9), as well as ζ_n . It is interesting to check the theoretical prediction (19). For the purpose we plotted the difference $\zeta_n - \eta_n$ as a function of n , see Fig. 10. For comparison, the theoretical straight line $n - 1$ (correct in $2d$) is drawn in the same figure. We see a good agreement, confirming the scaling (10) of the passive scalar correlation length $l(z)$ along the wall.

IV. CONCLUSION

We performed extensive numerical simulations of the passive scalar mixing in peripheral regions of random flows like high-Reynolds turbulence. The simulations confirm earlier theoretical expectations and reveal a lot of new details. At advanced stages of the passive scalar mixing passive scalar fluctuations are concentrated mainly in the narrow diffusive layer near the boundary provided the Peclet or the Schmidt number is large. We found that the passive scalar transport from the diffusive boundary layer to bulk is related to passive scalar tongues formed by jets directed to bulk. The tongues are objects responsible for strong intermittency characteristic of the passive scalar transport through the peripheral region.

We examined the passive scalar statistics outside the diffusive boundary layer and realized that both, moments of the passive scalar θ and of the passive scalar integrated along the wall, Θ , possess well pronounced scaling in terms of the separation from the wall z . We compared the corresponding exponents extracted from our numerics with our theoretical scheme and established their agreement. However, one should be careful since our theoretical predictions are correct for an infinite vessel and can be violated for the numerics where the velocity correlation length along the wall coincide with the velocity period. We found also an agreement between the theoretical prediction for the tongue cross-section dependence on z and our numerics. Therefore the simulations confirm our theoretical predictions.

There remain some problems to be solved in future. We are going to extend our consideration incorporating average flows (like in pipes) which are shear-like near the wall. Another natural extension of our approach is related to chemical reactions in random flows. One can also note polymer solutions, where the polymer elongation is very sensitive to the character of the flow. The problem is significant, e.g., for the elastic turbulence. However, a long-time memory characteristic of the polymer solutions could modify our results. We considered smooth walls in our work. There is a set of questions related to roughness of the wall, possible corners, caverns and peaks. All the objects can modify our conclusions, it is a subject of special investigation.

Our results agree qualitatively with data known from investigations of turbulent plumes in turbulent flows where a complicated space structure of the passive scalar fluctuations is observed [27–31]. We believe that statistical properties of the structure can be explained on the basis of our results implying production of the passive scalar tongues pushing to bulk. The explanation needs a generalization of our scheme where turbulent velocity fluctuations in bulk should be included. That is a subject of future work.

Acknowledgments

We thank M. Chertkov, I. Kolokolov, V. Steinberg and K. Turitsyn for numerous helpful discussions. Simulations were performed on the cluster Parma at the Lan-

dau Institute for theoretical physics RAS and the NGU cluster. The work was partly supported by RFBR grant 09-02-01346-a and by Russian Federal target program Kadry.

-
- [1] A. M. Obukhov, *Izv. Akad. Nauk. SSSR, Ser. Geogr. and Geophys.* **13**, 58 (1949).
 - [2] S. Corrsin, *J. Appl. Phys.* **22**, 469 (1951).
 - [3] A. N. Kolmogorov, *Dokl. Akad. Nauk. SSSR* **32**, 16 (1941).
 - [4] K. R. Sreenivasan, *Phys. Fluids* **8**, 189 (1996).
 - [5] Z. Warhaft, *Annu. Rev. Fluid Mech.* **32**, 203240 (2000).
 - [6] J. Schumacher and K. R. Sreenivasan, *Phys. Fluids* **17**, 125107 (2005).
 - [7] R. J. Miller, L. P. Dasi, and D. R. Webster, *Experiments in Fluids* **44**, 719 (2008).
 - [8] A. S. Monin and A. M. Yaglom, *Statistical Fluid Mechanics*, MIT Press, Cambridge, Mass. (1975).
 - [9] M. Lesieur, *Turbulence in Fluids*, Kluwer, Dordrecht, Netherlands, 3rd ed., (1997).
 - [10] U. Frisch, *Turbulence: the Legacy of A. N. Kolmogorov*, Cambridge University Press, New York (1995).
 - [11] J. M. Ottino, *The Kinematics of Mixing: Stretching, Chaos, and Transport* Cambridge University Press, Cambridge, England (1989).
 - [12] A. Groisman and V. Steinberg, *Nature* **405**, 53 (2000); *Phys. Rev. Lett.* **86**, 934 (2001); *Nature* **410**, 905 (2001).
 - [13] V. Kantsler and V. Steinberg, *Phys. Rev. Lett.* **95**, 258101 (2005).
 - [14] K. Gawędzki and A. Kupiainen, *Phys. Rev. Lett.* **75**, 3608 (1995).
 - [15] B. Shraiman and E. Siggia, *CRAS* **321**, Ser. II, 279 (1995).
 - [16] M. Chertkov, G. Falkovich, I. Kolokolov and V. Lebedev, *Phys. Rev. E* **52**, 4924 (1995).
 - [17] B. I. Shraiman and E. D. Siggia, *Review Nature (London)* **405**, 639 (2000).
 - [18] G. Falkovich, K. Gawędzki, and M. Vergassola, *Rev. Mod. Phys.* **73**, 913 (2001).
 - [19] T. Burghlea, E. Segre and V. Steinberg, *Phys. Fluids* **19**, 053104 (2007).
 - [20] M. Chertkov and V. Lebedev, *Phys. Rev. Lett.* **90**, 034501 (2003).
 - [21] M. Chertkov and V. Lebedev, *Phys. Rev. Lett.* **90**, 134501 (2003).
 - [22] V. V. Lebedev and K. S. Turitsyn, *Phys. Rev. E* **69**, 036301 (2004).
 - [23] T. Burghlea, E. Serge, and V. Steinberg, *Phys. Rev. Lett.* **92**, 164501 (2004).
 - [24] M. Chertkov, I. Kolokolov, and V. Lebedev, *Phys. Fluids* **19**, 101703 (2007).
 - [25] E. Balkovsky, G. Falkovich, V. Lebedev, and M. Lysiansky, *Phys. Fluids* **11**, 2269 (1999).
 - [26] A. Chernykh and V. Lebedev, *Pis'ma v ZhETF* **87**, 782 (2008) [*JETP Letters* **87**, 682 (2008)].
 - [27] J.-Y. Vincont, S. Simoens, M. Ayrault, and J. M. Wallace, *J. Fluid Mechanics*, **424**, 127 (2000).
 - [28] J. P. Crimaldi, M. B. Wiley, and J. R. Koseff, *J. Turbulence* **3**, 014 (2002).
 - [29] J. P. Crimaldi and J. R. Koseff, *Environ. J. Fluid Mech.* **6**, 573 (2006).
 - [30] J. P. Crimaldi, J. R. Koseff, and S. G. Monismith, *Phys. Fluids* **18**, 095102 (2006).
 - [31] L. P. Dasi, F. Schuerg, and D. R. Webster, *J. Fluid Mech.* **588**, 253277 (2007).